

The Influence of Size and Exposure Duration of Gold Nanoparticles on Gold Nanoparticles Levels in Several Rat Organs *In vivo*

Mohamed Anwar K Abdel Halim*

Department of Physics and Astronomy, College of Science, King Saud University, Riyadh 11451, Saudi Arabia

Abstract

Background: The bioaccumulation and toxicity of Gold Nanoparticles (GNPs) in several organs of rats becomes of more necessity prior to using them in drug delivery, diagnostics, and treatment. The GNPs levels in several rat organs *in vivo* have not been previously documented. This study was aimed to evaluate the influence of size and exposure duration of GNPs on the GNPs levels in several organs of rats *in vivo*.

Methods: Thirty rats were divided into a control group (NG: n = 10), group 1 (G1A: infusion of 10 nm GNPs for 3 days; n = 5; G1B: 10 nm GNPs for 7 days; n = 5) and group 2 (G2A: 50 nm GNPs for 3 days; n = 5; G2B: 50 nm GNPs for 7 days; n = 5). 50 μ l of GNPs dissolved in aqueous solution were administered intraperitoneally every day for 3 and 7 days.

Results: The GNPs levels were evaluated in several rat organs by Inductively Coupled Plasma-Mass Spectroscopy (ICP-MS) and Atomic Absorption Spectroscopy (AAS). In comparison with the control group, the GNPs levels increased in all the examined organs with G1A, G1B, G2A and G2B. The highest percentage normalized increase in the liver and lung organs were 468.6% and 273.4%, respectively with 10 nm GNPs after administration period of 7 days. The highest percentage normalized increase in the kidney and heart organs were 258.7% and 242.6%, respectively with 10 nm GNPs for administration period of 3 days.

Conclusions: Our results might indicate that GNPs are mostly taken up and accumulate in organs, suggesting the toxic effects induced by the smaller GNPs. These conclusions are further supported by histological investigation suggesting that the highest toxic effects were induced by the smaller GNPs and related to the time exposure of GNPs.

Keywords: Gold nanoparticles; Size; Exposure duration; Rats; Toxicity; Inductive coupled plasma-mass spectrometry

Introduction

The use of GNPs for detecting and treating the cancer is a new and exciting field of research. The current methods of cancer diagnosis and treatment are costly and can be harmful to the body. GNPs, however, offer an inexpensive route to targeting the cancerous cells [1].

GNPs are particularly promising since they are relatively easy to be produced in various shapes and can be conjugated with peptides/proteins for targeting to specific molecules [2]. In addition, GNPs undergo plasmon resonance when excited by light [3], whereby the gold electrons resonate in response to the incoming radiation, causing them to both absorb and scatter light.

The small size of GNPs implies that they could get close to a biological target of interest. Metallic GNPs can resonate in response to a time-varying magnetic field, which has certain advantages related to the particle energy transfer [3-7].

The particle size-dependent distribution of GNPs by organ has been studied *in vivo* [8-11]. Orally administered GNPs appeared in various organs in mice and the absorbance and distribution was inversely correlated with particle size [8]. The small size of GNPs results in physical and chemical properties that are very different from those of the same material in the bulk form. These properties include a large surface to volume ratio, enhanced or hindered particle aggregation depending on the type of surface modification, enhanced photoemission, high electrical and heat conductivity, and improved surface catalytic activity [12-16].

The GNPs levels in several rat organs are not documented and have

not yet been identified. In the present study, an attempt has been made to characterize the GNPs levels in the liver, kidney, heart and lung organs following experimental GNPs and, if so, whether are related to the size of these NPs and the time of exposure.

The present study was carried out to investigate the particle-size and exposure duration of GNPs on several rat organs in an attempt to cover and understand the toxicity and their potential therapeutic and diagnostic use. There is little *in vivo* data available regarding the levels of GNPs as a diagnostic tool for bioaccumulation of GNPs in rat organs. To explore the potential role of GNPs in therapeutic and diagnostic applications, we evaluated the levels of different GNPs sizes for periods of 3 and 7 days following intraperitoneal administration in rat.

Materials and Methods

GNP size

GNPs of different sizes (10 and 50 nm; MKN-Au-010 and MKN-

*Corresponding author: Mohamed Anwar K Abdel halim, Associate Professor, Department of Physics and Astronomy, College of Science, King Saud University, P.O. 2455, Riyadh 11451, Saudi Arabia, E-mail: abdelhalimmak@yahoo.com, mabdulhleem@ksu.edu.sa

Received April 30, 2012; Accepted July 03, 2012; Published July 05, 2012

Citation: Abdel Halim MAK (2012) The Influence of Size and Exposure Duration of Gold Nanoparticles on Gold Nanoparticles Levels in Several Rat Organs *In vivo*. J Cell Sci Ther 3:129. doi:10.4172/2157-7013.1000129

Copyright: © 2012 Abdel Halim MAK. This is an open-access article distributed under the terms of the Creative Commons Attribution License, which permits unrestricted use, distribution, and reproduction in any medium, provided the original author and source are credited.

Au-050, respectively; M K Impex Corp. MKNano 6382 Lisgar Drive Mississauga, Ontario L5N 6X1, CANADA) were purchased and used in this study. The mean size and morphology of GNPs were evaluated using the Transmission Electron Microscopy (TEM).

Animals

Healthy, male Wistar-Kyoto rats were obtained from the Laboratory Animal Center (College of Pharmacy, King Saud University). The rats were 8–12 weeks old (approximately 250 g body weight) and housed in pairs in humidity and temperature-controlled ventilated cages on a 12 h day/night cycle. Thirty rats were divided into a control group (NG: n = 10), group 1 (G1A: infusion of 10 nm GNPs for 3 days; n = 5; G1B: 10 nm GNPs for 7 days; n = 5) and group 2 (G2A: 50 nm GNPs for 3 days; n = 5; G2B: 50 nm GNPs for 7 days; n = 5). 50 μ l of GNPs dissolved in aqueous solution were only administered intraperitoneally to the rat treated-groups (G1A, G1B, G2A and G2B) for 3 and 7 days; while the control rat group left alone without administration of GNPs and/or aqueous solution.

The rats were anesthetized by inhalation of 5% isoflurane until they exhibited relaxed muscular tonus. Liver, heart, kidney and lung organs were collected from each rat. All experiments were conducted in accordance with the guidelines approved by the King Saud University Local Animal Care and Use Committee.

Digestion of rat organ samples

Various rat organ samples were wet digested with nitric acid and converted into acidic digest solutions for analysis by AAS and ICP-MS methods. The organ was freeze dried in order to minimize loss of analytes and to facilitate subsequent sample preparation steps, and then homogenized to a fine powder by ball-milling in plastic containers. Organ samples were dried completely in a clean oven at 60–70°C. Each dried organ was digested to white ash using 30% hydrogen peroxide (Powell, OH) at 50–60°C followed by digestion with concentrated ultra-pure trace-metal free nitric acid (0.1 ml, GFS Chemicals). Approximately 0.20 to 0.25 g of powdered organ was weighed into a Teflon reaction vessel and 3 ml of HNO₃ were added. The closed reaction vessel was heated in a 130°C oven until the digestion was completed. The samples were then diluted to a final volume of 20 ml with quartz distilled water and stored in 1 oz. polyethylene bottles for later analysis by the instrumental techniques.

Atomic absorption spectrophotometer (AAS) measurement

AAS determines the presence and concentration of gold (μ g/L) in the different organs of rats. The gold absorbed ultraviolet (UV) light when it was excited by heat. The AAS instrument looks for the gold by focusing a beam of UV light at a specific wavelength through a flame and into a detector. The sample of interest was aspirated into the flame. If the gold is present in the sample, it will absorb some of the light, thus reducing its intensity. The instrument measures the change in intensity. A computer data system converted the change in intensity into an absorbance. As the concentration goes up, the absorbance also goes up. A calibration curve was constructed by running standards of various concentrations (10, 15 and 20 PPM) on the AAS and the corresponding absorbance was observed. The samples were tested and measured against this curve. AAS measurements were carried out at the Research Center of King Saud University. The gold levels were measured using a Specter AA-220 series double-beam digital atomic

absorption spectrophotometer. The concentration of gold in each organ sample was calculated by comparing the absorbance produced by the sample with that produced by a series of standards [17].

Inductively coupled plasma-mass spectrometry (ICP-MS)

A PlasmaQuad-3 ICP-MS instrument (V.G Elemental, Cheshire, UK) was used to quantify gold in the digested organ samples. This instrument uses an 8000°C temperature radio frequency-generated argon plasma to atomize and ionize gold ions to singly charged mass ions and the mass-to-charge (m/z) ratio signals were used to quantify the elements. Bismuth (209Bi) 1 ng/mL, was added to all samples as an internal standard in order to correct errors due to instrument drifts during data acquisitions. The digested samples were diluted suitably using 1% nitric acid, aspirated and then nebulized using a quartz Meinhard micro-concentric type nebulizer into the argon plasma via a peristaltic pump with a flow rate of approximately 0.9–1.0 mL/min. Mass spectral acquisitions were carried out using pulse-counting scanning mode with the following instrumental parameters: mass range scanned 190–220 m/z with 19 channels per mass, three points per peak, and 10.24 ms dwell time on each isotopic mass. The instrument control, methods procedures, and the data system, including calculations and statistics were operated via a personal computer with Plasma Vision Software. Nitric acid (1%) blanks were run in between samples to correct the background levels [18].

Statistical analysis

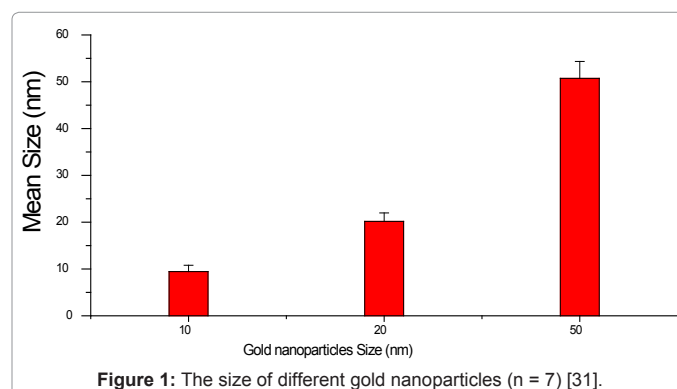
To assess the significance of differences between the control and the 4 test groups (G1: 10 nm; G2: 50 nm; A: infusion of 50 μ l GNPs for 3 days; B: infusion of 50 μ l GNPs for 7 days), the statistical analysis was performed using one-way analysis of variance (ANOVA) for repeated measurements. The significance was assessed at a 5% confidence level.

Results and Discussion

Size and morphology of GNPs

The mean sizes for 10 and 50 nm GNPs were calculated from the TEM images. Mean size for 10 nm GNPs was 9.45 ± 1.33 nm and 50 nm GNPs was 50.73 ± 3.58 nm (Figure 1) [19]. The 10 nm GNPs show spherical morphology; while the 50 nm GNPs show hexagonal morphology. All GNPs show narrow particle size distribution and good dispersion in the solution (Figure 2) [20,21].

To determine accurate distribution of GNPs in rat several organs, we employed two different techniques to measure the gold levels in various organs, including liver, kidney, heart, and lungs. With both



ICP-MS and AAS, the amounts of gold detected in each organ were different. After the intraperitoneal administration of 10 and 50 nm GNPs at the dose of 50 μ l for 3 and 7 days, we found significant increase of gold levels in the several organs examined (Figures 1- 4), suggesting that the administrated GNPs were absorbed into systemic circulation and distributed into organs.

GNPs-normal rat demonstrating normal GNPs levels as shown in Figures 1-4. In comparison with the control group, the alterations of GNPs levels were detected in the liver (Figure 1), heart (Figure 2), lung (Figure 3) and kidney (Figure 4) of GNPs treated rats. The GNPs levels significantly increased in all the examined organs with G1A, G1B, G2A and G2B compared with the control.

The percentage normalized increase in liver organ with G1A, G1B, G2A and G2B was 246%, 468.6%, 264.4 and 290%, respectively (Figure 3). Figure 3 indicates that the highest percentage normalized increase in liver organ was 468.6% with 10 nm GNPs for administration period of 7 days.

The percentage normalized increase in heart organ with G1A, G1B, G2A and G2B was 242.6%, 31.7%, 82.5% and 96.5%, respectively (Figure 4). Figure 4 indicates that the highest percentage normalized increase in heart organ was 242.6% with 10 nm GNPs for administration period of 3 days.

The percentage normalized increase in lung organ with G1A, G1B, G2A and G2B was 124.8%, 273.4%, 84.9% and 17.7%, respectively (Figure 5). Figure 5 indicates that the highest percentage normalized increase in lung organ was 273.4% with 10 nm GNPs for administration period of 7 days.

The percentage normalized increase in kidney organ with G1A, G1B, G2A and G2B was 258.7%, 256.6%, 200.5% and 110.6%, respectively (Figure 6). Figure 6 indicates that the highest percentage normalized increase in kidney organ was 258.7% with 10 nm GNPs for administration period of 3 days.

It became evident from these results that the alterations in GNPs levels were size-dependent with smaller ones induced the most toxicity effects and related with time exposure of GNPs as shown in Figures 1 and 3 (liver and lung organs).

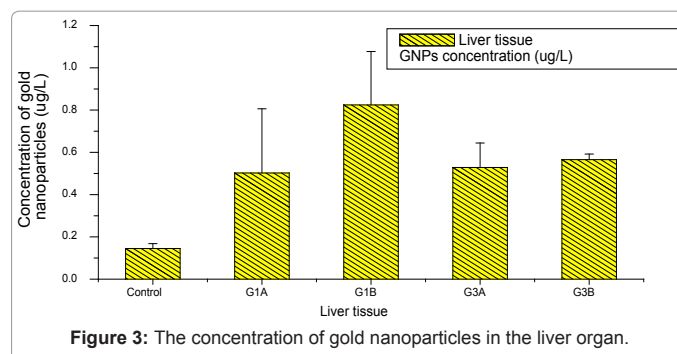


Figure 3: The concentration of gold nanoparticles in the liver organ.

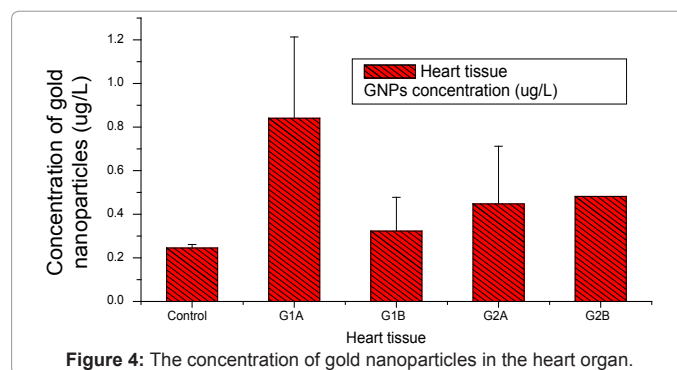


Figure 4: The concentration of gold nanoparticles in the heart organ.

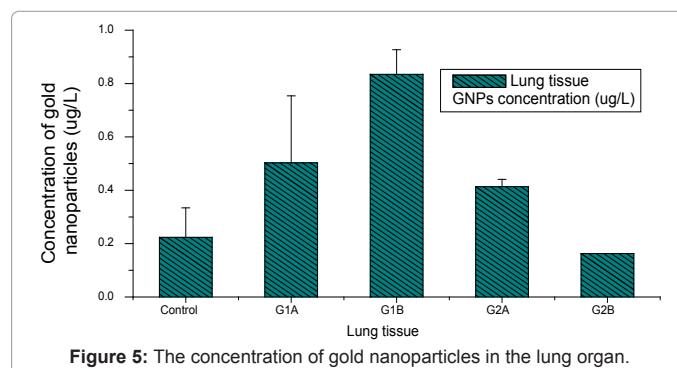


Figure 5: The concentration of gold nanoparticles in the lung organ.

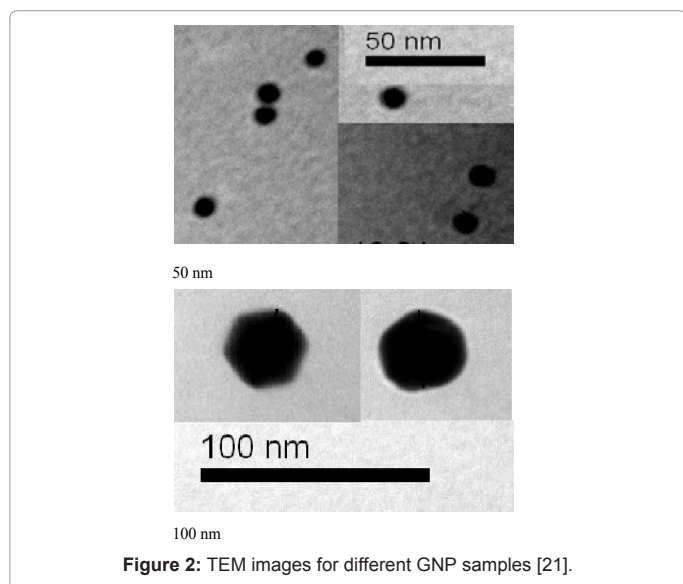


Figure 2: TEM images for different GNP samples [21].

The increase in GNPs levels might be an indication of injured hepatocytes due to GNPs toxicity that became unable to deal with the accumulated residues resulting from metabolic and structural disturbances caused by these NPs [22-25]. It has been reported that the gold levels in blood were not indicate significant difference after 8 days of administration of GNPs; while the bioaccumulation of GNPs in the brain was significantly increased in a dose-dependent manner with higher levels than the reported physiological levels in brain [26].

No significant differences were observed for any of the organs studied as compared with controls untreated animals. These observations indicate that extensive inflammation might not be induced in the mice after administration of gold nanoparticles, which is confirmed by the macroscopic morphological examination described later.

Cho et al. [27] have demonstrated that the organ gold concentration is time dependent after injection, and after intravenous injection of 13 nm GNPs, the gold was found in various organs just 3 day after injection. However, the blood gold levels not increased in proportional

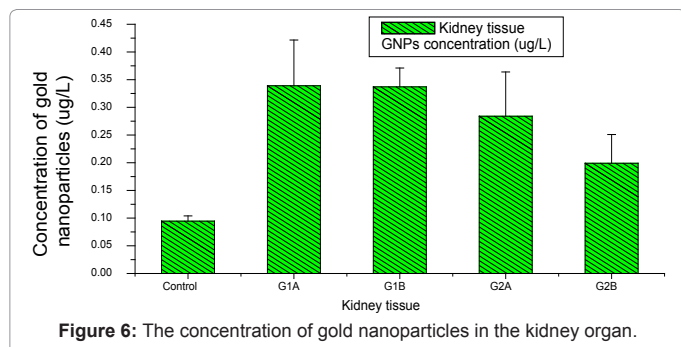


Figure 6: The concentration of gold nanoparticles in the kidney organ.

Product # MKN	Product # MKN-Au-010	Product # MKN-Au-050
Size (nm)	10 nm	50 nm
Concentration of Au	0.01% Au	0.01% Au
Number of particles (particles/ml)	5.7×10^{12}	4.5×10^{10}

Table 1: Gold nanoparticles in aqueous solution.

to the dose, indicating that GNPs are taken up and accumulate in organs.

In this study, the lowest percentage normalized increase of the smaller GNPs in the kidney organs compared with the liver and lung organs could be explained by the bigger size of the GNP s with respect to the glomerular pores that nearly measure 6 nm. So it is unlikely that NPs can pass through the glomerular filtration due to its size and negative electrostatic potential. The lowest percentage normalized increase of the larger GNPs compared with the smaller GNPs might be attributed to the highly excretion of GNPs via the hepatobiliary system into the feces. The bioaccumulation and toxicity induced by the GNPs are particle size, exposure duration and surface characteristics dependent.

The bioaccumulation of GNPs in the spleen and liver organs may be regulated by the reticulo-endothelial system involved in the uptake and metabolism of exogenous molecules and particles in these organs, and the NPs are taken up by kupffer cells in the liver and by macrophages in other place regardless of the particle size [28].

Abdelhalim, 2011 and 2012 [29-31] and Abdelhalim and Jarrar, 2011 [24,25] have published several articles related to the histological alterations in several rat organs, and indicated that the amount of accumulated GNPs in the organ reflected the toxicity. The induced histological alterations have been observed in several rat organs. These histological alterations were size-dependent with smaller ones induced the most effects and related with time exposure of GNPs.

The administration of GNPs induced in the liver: prominent inflammatory, central vein intima disruption, fatty change and Kupffer cells hyperplasia. In addition to induced cloudy swelling to hydropic degeneration, cytoplasmic hyaline vacuolation, polymorphism, binucleation, karyopyknosis, karyolysis, karyorrhexis and necrosis [24,25]; in the kidney organ: renal cells cytoplasmic degeneration and nuclear destruction) [24,25]; in the heart organ: disarray of heart muscle, hemorrhagic, chronic inflammatory cells infiltrated by small lymphocytes, cytoplasmic vacuolization and congested and dilated blood vessels. In addition to cardiac organ damage [29,30]; in the

lung organ: pneumonia, fibrosis, chronic inflammatory cell infiltrates, congested and dilated blood vessels, and hemosiderin granule and emphysema foci [31].

Hepatocytes exhibited cloudy swelling accompanied by leakage of lysosomal hydrolytic enzymes, which resulted in cytoplasmic degeneration and macromolecular crowding, and ballooning degeneration. These changes were more prominent with 10 nm size particles than with larger ones. This may be the result of disturbances in membrane function, leading to water and Na^+ influx [23,24,27].

Mice exposed to GNPs showed no organ damage in any of the sections obtained from the kidney, liver, spleen, brain or lungs. Accumulation of GNPs in different organs did not induce toxicity as assessed by animal behavior, organ morphology, and histopathological examination [26].

The bioaccumulation of GNPs in the liver organ may be regulated by the reticuloendothelial system, which is part of the immune system involved in the uptake and metabolism of exogenous molecules and particles. In addition, GNPs are taken up by kupffer cells in the liver and by macrophages in other organs, regardless of the particle size [24,25,28].

Conclusions

The GNPs levels were evaluated in several rat organs by inductively coupled plasma-mass spectroscopy (ICP-MS) and atomic absorption spectroscopy (AAS). In comparison with the control rats, the GNPs levels increased in all the examined organs with G1A, G1B, G2A and G2B. The highest percentage normalized increase in the liver and lung organs were 468.6% and 273.4%, respectively with 10 nm GNPs after administration period of 7 days. The highest percentage normalized increase in the kidney and heart organs were 258.7% and 242.6%, respectively with 10 nm GNPs for administration period of 3 days.

It became evident from the results of this study that the alterations in GNPs levels were size-dependent with the smaller ones induced the most toxicity effects and related with the time exposure of GNPs (liver and lung organs). Our results might indicate that GNPs are mostly taken up and accumulate in organs, suggesting the toxic effects induced by the smaller GNPs.

These conclusions are further supported by histological investigation suggesting that the highest toxic effects were induced by the smaller GNPs and related to the time exposure of GNPs.

Authors' Contributions

MAKA analyzed and data and wrote the final draft of the manuscript. The animal model used in this study was obtained from the Laboratory Animal Center (College of Pharmacy, King Saud University). MAKA conceived the study and design, and obtained the research grants that supported the study. The author has read and approved the final manuscript.

Acknowledgements

The author is very grateful to NPST. The National Science and Technology Innovation Plan (NSTIP) provided funding for this project through Research No. 08-ADV206-02 and Research No. 09-NAN670-02, College of Science, King Saud University, Saudi Arabia.

References

- Caruthers SD, Wickline SA, Lanza GM (2007) Nanotechnological applications in medicine. *Curr Opin Biotechnol* 18: 26-30.
- Liu WT (2006) Nanoparticles and their biological and environmental applications. *J Biosci Bioeng* 102: 1-7.

3. Pellequer Y, Lamprecht A (2009) Nosancale cancer therapeutics. In Lamprecht A (Eds), *Nanotherapeutics: Drug delivery concepts in nanoscience*. Chicago: Pan Stanford Publishing 93-124.
4. Garg J, Poudel B, Chiesa M, Gordon JB, Ma JJ, et al. (2008) Enhanced thermal conductivity and viscosity of copper nanoparticles in ethylene glycol nanofluid. *J Appl Phys* 103: 301.
5. McNeil SE (2005) Nanotechnology for the biologist. *J Leukoc Biol* 78: 585-594.
6. Rosi NL, Mirkin CA (2005) Nanostructures in biodiagnostics. *Chem Rev* 105: 1547-1562.
7. Shrestha S, Yeung MY, Nunnerley C, Tsang SC (2007) Comparison of morphology and electrical conductivity of various thin films containing nano-crystalline praseodymium oxide particles. *Sens Actuators A Phys* 136: 191-198.
8. Kamat PV (2002) Photophysical, Photochemical and photocatalytic aspects of metal nanoparticles. *J Phys Chem B* 106: 7729-7744.
9. Kuwahara Y, Akiyama T, Yamada S (2001) Facile Fabrication of Photoelectrochemical Assemblies Consisting of Gold Nanoparticles and a Tris (2,2'-bipyridine) ruthenium (II)-Viologen Linked Thio Langmuir 17: 5714-5716.
10. Mirkin CA, Letsinger RL, Mucic RC, Storhoff JJ (1996) A DNA-based method for rationally assembling nanoparticles into macroscopic materials. *Nature* 382: 607-609.
11. Huber M, Wei TF, Müller UR, Lefebvre PA, Marla SS, et al. (2004) Gold nanoparticle probe-based gene expression analysis with unamplified total human RNA. *Nucleic Acids Res* 32: e137.
12. Kogan MJ, Olmedo I, Hosta L, Guerrero AR, Cruz LJ, et al. (2007) Peptides and metallic nanoparticles for biomedical applications. *Nanomedicine* 2: 287-306.
13. El-Sayed IH, Huang X, El-Sayed MA (2006) Selective laser photo-thermal therapy of epithelial carcinoma using anti-EGFR antibody conjugated gold nanoparticles. *Cancer Lett* 239: 129-135.
14. Kogan MJ, Bastus NG, Amigo R, Grillo-Bosch D, Araya E, et al. (2006) Nanoparticle-mediated local and remote manipulation of protein aggregation. *Nano Lett* 6: 110-115.
15. Zharov VP, Mercer KE, Galitovskaya EN, Smeltzer MS (2006) Photothermal nanotherapeutics and nanodiagnostics for selective killing of bacteria targeted with gold nanoparticles. *Biophys J* 90: 619-627.
16. Hirsch LR, Stafford RJ, Bankson JA, Sershen SR, Rivera B, et al. (2003) Nanoshell-mediated near-infrared thermal therapy of tumors under magnetic resonance guidance. *Proc Natl Acad Sci U S A* 100: 13549-13554.
17. Abdelhalim MA, Alhadlaq HA, Moussa SA (2010) Elucidation of the effects of a high fat diet on trace elements in rabbit tissues using atomic absorption spectroscopy. *Lipids Health Dis* 9: 2.
18. De Jong WH, Hagens WI, Krystek P, Burger MC, Sips AJ, et al. (2008) Particle size-dependent organ distribution of gold nanoparticles after intravenous administration. *Biomaterials* 29: 1912-1919.
19. Abdelhalim MA, Jarrar BM (2012) Histological alterations in the liver of rats induced by different gold nanoparticle sizes, doses and exposure duration. *J Nanobiotechnology* 10: 5.
20. Abdelhalim MA, Mady MM, Ghannam MM (2012) Physical properties of different gold nanoparticles: ultraviolet-visible and fluorescence measurements. *J Nanomedic Nanotechnol* 3: 133.
21. Abdelhalim MA, Mady MM (2011) Liver uptake of gold nanoparticles after intraperitoneal administration in vivo: a fluorescence study. *Lipids Health Dis* 10: 195.
22. Abdelhalim MA, Jarrar BM (2011) Gold nanoparticles administration induced prominent inflammatory, central vein intima disruption, fatty change and Kupffer cells hyperplasia. *Lipids Health Dis* 10: 133.
23. Abdelhalim MA, Jarrar BM (2011) Gold nanoparticles induced cloudy swelling to hydropic degeneration, cytoplasmic hyaline vacuolation, polymorphism, binucleation, karyopyknosis, karyolysis, karyorrhexis and necrosis in the liver. *Lipids Health Dis* 10: 166.
24. Abdelhalim MA, Jarrar BM (2011) The appearance of renal cells cytoplasmic degeneration and nuclear destruction might be an indication of GNPs toxicity. *Lipids Health Dis* 10: 147.
25. Abdelhalim MA, Jarrar BM (2011) Renal tissue alterations were size-dependent with smaller ones induced more effects and related with time exposure of gold nanoparticles. *Lipids Health Dis* 21: 163.
26. Lasagna-Reeves C, Gonzalez-Romero D, Barria MA, Olmedo I, Clos A, et al. (2010) Bioaccumulation and toxicity of gold nanoparticles after repeated administration in mice. *Biochem Biophys Res Commun* 393: 649-655.
27. Cho WS, Cho M, Jeong J, Choi M, Cho HY, et al. (2009) Acute toxicity and pharmacokinetics of 13 nm-sized PEG-coated gold nanoparticles. *Toxicol Appl Pharmacol* 236: 16-24.
28. Sadauskas E, Wallin H, Stoltenberg M, Vogel U, Doering P, et al. (2007) Kupffer cells are central in the removal of nanoparticles from the organism. *Part Fibre Toxicol* 4: 10.
29. Abdelhalim MA (2011) Gold nanoparticles administration induces disarray of heart muscle, hemorrhagic, chronic inflammatory cells infiltrated by small lymphocytes, cytoplasmic vacuolization and congested and dilated blood vessels. *Lipids Health Dis* 10: 233.
30. Abdelhalim MA (2011) Exposure to gold nanoparticles produces cardiac tissue damage that depends on the size and duration of exposure. *Lipids Health Dis* 10: 205.
31. Abdelhalim MA (2012) Exposure to gold nanoparticles produces pneumonia, fibrosis, chronic inflammatory cell infiltrates, congested and dilated blood vessels, and hemosiderin granule and emphysema foci. *J Cancer Sci Ther* 4: 046-050.